Polymer Chain Conformation and Dynamical Confinement in a Model One-Component Nanocomposite

C. Mark,[1] O. Holderer,[2] J. Allgaier,[1] E. Hübner,[1,*] W. Pyckhout-Hintzen,[1] M. Zamponi,[2] A. Radulescu,[2] A. Feoktystov,[2] M. Monkenbusch,[1] N. Jalarvo,[3,†] and D. Richter[1]

[1]*Jülich Centre for Neutron Science (JCNS) and Institute for Complex Systems (ICS), Forschungszentrum Jülich GmbH, 52425 Jülich, Germany*

[2]*Forschungszentrum Jülich GmbH, JCNS at Heinz Maier-Leibnitz Zentrum (MLZ), Lichtenberstraße 1, 85747 Garching, Germany*

[3]*Forschungszentrum Jülich GmbH, JCNS at SNS-Oak Ridge National Laboratory (ORNL), 1 Bethel Valley Road, Oak Ridge, Tennessee 37831, USA*

(Received 2 March 2017; published 26 July 2017)

We report a neutron-scattering investigation on the structure and dynamics of a single-component nanocomposite based on SiO_2 particles that were grafted with polyisoprene chains at the entanglement limit. By skillful labeling, we access both the monomer density in the corona as well as the conformation of the grafted chains. While the corona profile follows a r^{-1} power law, the conformation of a grafted chain is identical to that of a chain in a reference melt, implying a high mutual penetration of the coronas from different particles. The brush crowding leads to topological confinement of the chain dynamics: (i) At local scales, the segmental dynamics is unchanged compared to the reference melt, while (ii) at the scale of the chain, the dynamics appears to be slowed down; (iii) by performing a mode analysis in terms of end-fixed Rouse chains, the slower dynamics is tracked to topological confinement within the cone spanned by the adjacent grafts; (iv) by adding 50% matrix chains, the topological confinement sensed by the grafted chain is lifted partially and the apparent chain motion is accelerated. We observe a crossover from pure Rouse motion at short times to topological confined motion beyond the time when the segmental mean squared displacement has reached the distance to the next graft.

DOI: 10.1103/PhysRevLett.119.047801

Recently, polymer hybrids such as the novel one-component nanocomposites (OCNCs) have drawn much attention both in basic as well as in application-oriented research [1,2]. OCNCs consist of nanoparticles that are grafted with polymer chains without any matrix chains. Progress in chemistry facilitates the precise creation of materials with well-defined grafting density, chain length, and functionalization [3]. These OCNCs exhibit novel morphologies, dielectric, and mechanical properties, overcome the dispersion challenge, and are expected to display structure-related *emergent* properties that distinguish them from the more established field of nanocomposites [1]. OCNCs have been proposed for energy storage in supercapacitors [4], for precise manufacturing of tunable hypersonic photonic crystals [5], as particle-brush building blocks for self-healing materials [6], etc. In biomedicine, envisaged applications are, e.g., polypeptide-based hybrids for drug carriers or building blocks for tissue engineering [7]. The mechanical properties depend strongly on the grafted chain length; long chains in OCNCs dramatically increase the toughness and flexibility of *particle solids* [8] as well as the fracture resistance [8]. The increased toughness enables the fabrication of ordered films and bulk structures [9] with a high potential for the creation of functional materials. Substrate-induced ordering leads to OCNC films that display anisotropic elasticity [10], opening the opportunity to fabricate mechanically strongly anisotropic materials.

Even though OCNCs promise a plethora of novel applications, the understanding of their properties is still in its infancy. Describing the polymer conformation in terms of a mean field model, Kumar predicted a stretched inner concentrated polymer brush with the brush height $h \propto N^{4/5}$ and a relaxed outer semidilute polymer brush with $h \propto N^{3/5}$ (N the number of segments) [11], while for low grafting density $\kappa < 1/R_g^2$ (R_g the radius of gyration), mushroomlike conformations with $h = 2R_g$ are prevailing. For spherical brushes, corrections were given by Milner, Witten, and Cates [12] and Wijmans and Zhulina [13]. Experiments are available in solution only, from which conclusions on the scaling behavior of the hydrodynamic radius were drawn [11]. The rheology and flow behavior are largely unexplored [2], and nothing is known about the dynamics on the chain level.

We present a neutron-scattering study on the structure and dynamics of an OCNC based on SiO_2 particles grafted with polyisoprene (PI) chains at the entanglement limit. The following results stand out. (i) The grafted chain conformation statistics and R_g equal that of a reference melt. (ii) The nanoparticle (NP) corona profile decays with a r^{-1} power law. (iii) Though the local mobility is not affected by grafting, (iv) the dynamics on the chain level is severely reduced. (v) A quantitative analysis in terms of an end-fixed Rouse model reveals that the chain motion is

TABLE I. Polymer sample characteristics.

Polymers	h-PI	d-PI	Random copolymer
M_w	5000	5400	5100
M_n	4850	5300	5000
M_w/M_n	1.03	1.03	1.03

confined to a cone set by the adjacent grafts. (vi) Finally, diluting with matrix chains induces a crossover from unrestricted Rouse motion at early times to confined dynamics later on. (vii) The quantification of the confinement in OCNCs will have important ramification for an understanding of their rheology.

The single-component nanocomposite was based on SiO_2 nanoparticles from Nissan Chemical Industries ORGANOSILICASOL™. Their size distribution follows a log-normal distribution ($R_m = 6$ nm; $\sigma = 0.37$) with a fuzzy surface ($t = 0.3$ nm thickness); the scattering length densities were $\rho_{SiO_2} = 3.48 \times 10^{10}$ cm^{-2} and $\rho_{\text{fuzzy}} = -1.26 \times 10^{10}$ cm^{-2}, resulting in an average of $\rho_m = 3.13 \times 10^{10}$ cm^{-2} [14]. The polyisoprene (PI) polymers were synthesized by anionic polymerization with three different hydrogen or deuterium labeling and grafted to the particle surface; see Table I. The SiO_2 particles were first functionalized with $(CH_3)_2SiCl_2$ as a linker. Then living chains were added such that the h/d mixture (sample 1) or the decoration with the random copolymer (sample 2) was contrast matching the nanoparticle. Nonlinked chains were removed by fractionation, such that the remaining free chains amounted to less than 1%. The details of the functionalization procedure and particle properties are given in Ref. [15] and Supplemental Material [16]. Characterization was performed by elementary analysis with the result of an average number of chains per particle $\langle f \rangle = 364$ or 375 leading to a grafting density of $\kappa = 0.59$ nm^{-2}. We remark that at the matching condition about 10% of the protons are associated with the surface and are immobile.

The small-angle neutron-scattering (SANS) measurements—carried out at KWS1 at the MLZ in Garching, Germany [17]—aimed for the chain conformation of the grafted chains as well as for the form factor of the grafted particle. The form factor was obtained from sample 2 immersed in a protonated matrix at volume fractions: 0.01, 0.05, 0.15, 0.3, and 0.5. Background from h-PI and a random copolymer was measured separately and subtracted; at a sample transmission of 0.45, the necessary self-shielding correction was performed. The data were analyzed in terms of a core-shell particle based on results for a SiO_2 core including the fuzzy surface. The shell was modeled by a power law profile $r^{-\beta}$ (resulting in $\beta = 1$) that was combined with a Fermi cutoff function leading to a shell thickness of $t = 6$ nm. Based on the condition of equal free energy per

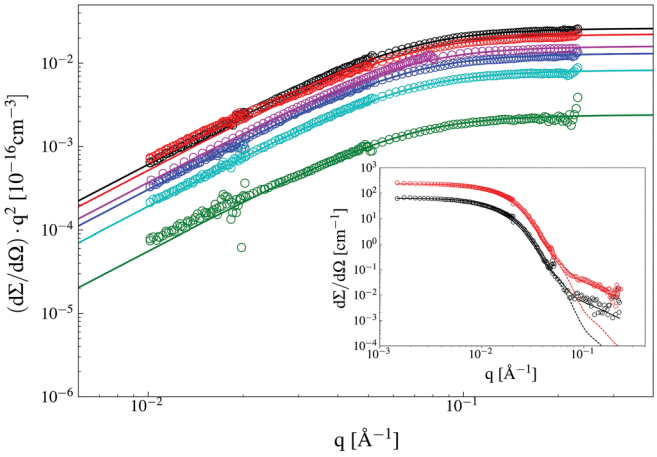

FIG. 1. Kratky plot of single-chain form factors from h/d mixed chain grafted particles in a melt of contrast matching random h/d copolymer including a Debye fit. Black, reference melt; red, 15 vol%; blue, 50 vol% melt; green, 15 vol%; teal, 50 vol%; violet, 100% grafted shell. The inset shows the particle form factor from random polymer grafted particles in a protonated melt (red, 5%; black, 1%) with model fits (solid lines) NP form factor plus the grafted chain scattering and (dashed lines) NP form factor only.

chain for all particles, surface curvature effects on the grafting density were included. The minimum free energy condition leads to a distribution of grafted chains depending on the particle size with a significantly higher grafting density for small particles; e.g., $\kappa = 1$ nm^{-2} for 3.6 nm radius; however, these small particles carry little weight in scattering, where 80% result from particles larger than $R = 7.2$ nm. There the grafting density $\kappa \leq 0.63$ nm^{-2} is close to average. The form factor and the achieved fit are shown as an inset in Fig. 1. More details of the form factor model are given in Supplemental Material [16]. The grafted chain conformation was obtained from sample 1 immersed in the random copolymer matrix; see the Kratky plot in Fig. 1. In all cases for the grafted chains as well as for the reference melt, perfect Debye form factors are observed displaying Q^{-2} power law asymptotes; for all situations, the radii of gyration $R_g = 2.17$ nm are identical; the end to end distance $R_e = 5.3$ nm and the shell thickness $t = 6$ nm are in good agreement. Obviously, the different chains strongly interpenetrate, no stretching is visible (Q^{-2} behavior), and chain collapse does not occur. The results are well explained in terms of a semidilute brush regime [11], where the brush height $h \propto (l_0 N \sigma^{1/3})^{3/5} = 5.3\,\text{nm}$ ($\kappa^* = \kappa l_0^2$; $l_0^2 = 3.84 C_\infty l^2 = 0.5$ nm^2) is predicted in good agreement with our evaluation; in addition, the self-consistent field theory by Dan and Tirell [18] showed that the grafted chain ends are uniformly distributed in the brush, corroborating the observed Debye behavior.

The segmental dynamics of the grafted chains was studied on sample 2 using neutron backscattering at the

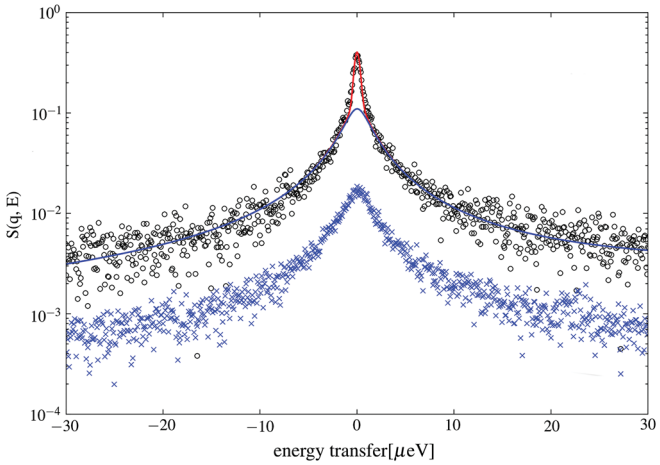

FIG. 2. Comparison of neutron backscattering spectra of the reference random polymer at $Q = 6$ nm^{-1} and $T = 348$ K with the grafted random copolymer chains at the same Q and T. (Solid line) Polymer melt spectrum plotted through the data from the grafted chains. The red line indicates an additional elastic peak contribution that results from residual core scattering including a small contribution of about 5% immobilized segments at the grafting sites on the surface.

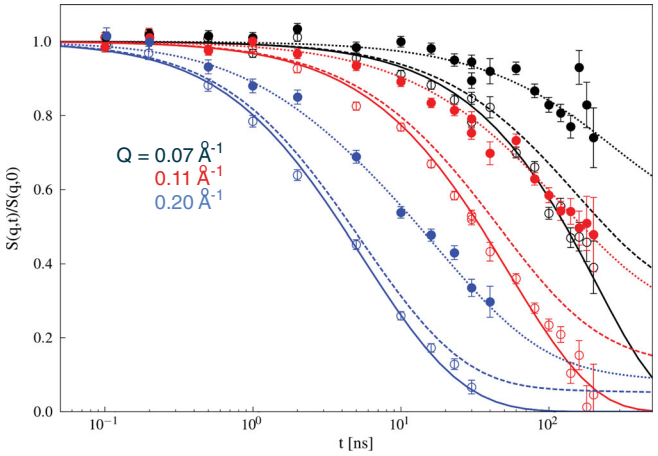

FIG. 3. Neutron spin-echo data from the reference polymer (open circles) together with the OCNC results (full circles) in one plot. Solid colored lines, Rouse model—agreeing very well with reference; dashed colored lines, end-fixed Rouse; and dotted colored lines, fit with reduced amplitudes agreeing well with the grafted sample.

instruments BASIS at the SNS in Oak Ridge [19] and SPHERES at MLZ in Garching [20]. Figure 2 compares spectra taken from a reference random polymer melt at $Q = 6$ nm^{-1} at $T = 348$ K with the grafted random copolymer chains at the same Q and T. The reference melt data were fitted with stretched exponentials. The solid line in Fig. 2 projects the pure melt result to the spectrum from the grafted chains. Aside from a small elastic peak contribution (red line) resulting from surface protons and some silica background and from a few segments near the grafting sites on the surface, the reference melt dynamics perfectly describes the local dynamics of the grafted chains. The resolution function used to model the spectra was taken from the data at 40 K, where all dynamic processes are frozen. Obviously, there is no effect of the grafting on the local segmental motion.

The dynamics at the chain level (sample 1) was accessed with the neutron spin echo (NSE) instrument at MLZ [21]. Figure 3 displays NSE data from the reference melt together with the results from sample 1 in one plot; evidently, the chain dynamics of the grafted chains is severely slowed down, even though the segmental motion is identical. The dynamics of unentangled chains in the melt to a good approximation can be described in terms of the Rouse model [22] that treats the dynamics of a Gaussian chain in a heat bath. Then only entropic forces originating from the conformational chain entropy drive the dynamics. The model is solved by modes p along the chain with mode relaxation times $\tau_p = R_e^4/(Wl_0^4\pi^2 p^2)$ and corresponding wavelengths $\lambda \simeq N/p$. The normalized single-chain dynamic structure factor $S(Q,t)_{\text{chain}}/S(Q,t=0)$ has the form

$$S(Q,t)/S(Q) = \sum_{n,m}^{N} \exp\left[-\frac{1}{6}Q^2 B(n,m,t)\right] \quad \text{with}$$
$$B(n,m,t) = 6D_R t + |n-m|l_0^2 + \frac{4R_e^2}{\pi^2}\sum_{p=1-s}^{N-s}\frac{A_p}{p^2}\cos\left(\frac{p\pi n}{N}\right) \times \cos\left(\frac{p\pi m}{N}\right)(1-e^{-t/\tau_p}) \quad (1)$$

with the *Rouse rate* $Wl_0^4 = 3k_B T l_0^2/\zeta_0$, where k_B is the Boltzmann constant, T the temperature, and ζ_0 the monomeric friction coefficient, the Rouse diffusion coefficient $D_R = Wl_0^4/(3R_e^2)$, and the mode amplitudes $A_p = 1$. For a chain in the melt $s = 0$, while for an end-fixed chain $s = 1/2$ and $D_R = 0$. This choice ensures that only such modes are allowed that exhibit a knot at the grafting point. We note that for $p = 1/2$ at short times $B_{p=1/2}(N/2, N/2, t) = 6D_R t$ describing the initial center of mass diffusion. A fit with the Rouse model for the chain melt resulted in the colored dashed lines with the only fit parameter $Wl_0^4 = 0.78 \pm 0.013$ nm^4/ns comparing well with the literature value of $Wl_0^4 = 0.83$ nm^4/ns [23]; the longest relaxation time $\tau_R = \tau_{p=1} = 104$ ns (Rouse time) was well within the observation window. We notice the very good quality of the data description. Using the end-fixed Rouse model to describe the grafted chain dynamics (dashed colored lines) fails. The NSE spectra might be well described using a very small Rouse rate: $Wl^4 = 0.21$ nm^4/ns. However, with the prior knowledge of the unchanged local dynamics, this is not a solution. Considering the possibility of topological confinement in a second approach, we have explored a reduction of

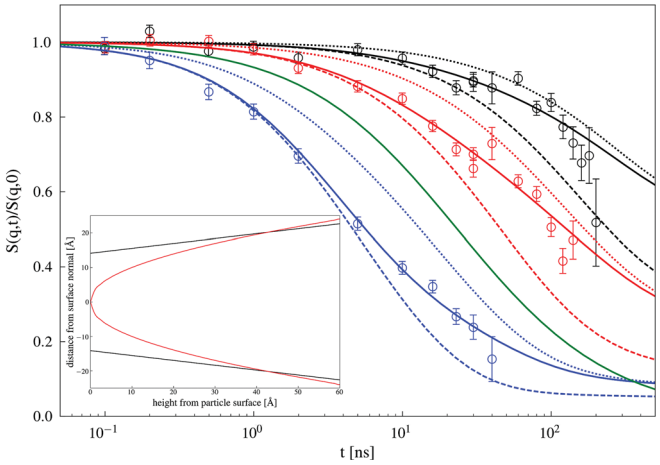

FIG. 4. Neutron spin-echo results from 50% grafted particles in a random copolymer melt (Q values as in Fig. 3). Dotted lines, dynamics of the OCNC sample; dashed lines, end-fixed Rouse model; full lines, crossover model from end-fixed to grafted dynamics; green line, Fermi crossover function. (Inset) Permitted average fluctuation range of a grafted chain in the OCNC from the grafting point to the rim of the corona; straight lines, cone set by the adjacent grafted chains.

mode amplitudes for long-wavelength Rouse modes. For this purpose, we modify the mode amplitudes $A_p = 1$ in Eq. (1) by an empirical cutoff function $A_p = \exp[(p-p_0)/\sigma]/\{\exp([p-p_0]/\sigma)+1\}$ and keep Wl_0^4 at its value for the reference melt. With $p_0 = 6 \pm 2; \sigma = 14 \pm 7$, this approach fits the data very well (Fig. 3; dotted lines) with mode amplitudes slowly rising from 0.4 at $p = 1/2$ to 0.47 at $p = 9/2$. We note that the large errors for p_0 and σ result from the fact that modes beyond $p = 4$ do not contribute significantly within the experimental Q window. Thus, grafting does not decelerate the segmental mobility by increasing the friction, but the topological chain-chain interactions create confinement: The amplitude of motion in different modes is strongly reduced.

In order to further investigate the confinement effects caused by crowding, we also studied a NC, where 50% NP grafted with a mixture of h/d PI was immersed in a melt of random copolymers, such that the particle as a whole was matched. Figure 4 displays the result: Compared to the OCNC (100% grafted particles, dotted lines), the dynamics is significantly enhanced but still is slower than the prediction of the end-fixed Rouse model (dashed lines). Note, however, that at short times $S(Q,t)/S(Q)$ seems to follow the (theoretical) unrestricted Rouse model of an end-fixed chain, while at long times it appears to change over to the restricted dynamics of the OCNC. Thus, the data display a time-dependent crossover between the two limiting behaviors that may be well empirically described by a logarithmic Fermi function $f(t) = 1/\{\exp[(\log t - \log t_0)/w] + 1\}$. The corresponding scattering function becomes

$$S(Q,t) = f(t)S(Q,t)_{\text{endfixed}} + [1 - f(t)]S(Q,t)_{\text{grafted}}. \quad (2)$$

A fit to the data gives excellent results revealing $t_0 = 22.4$ ns and $w = 1.2$ (solid lines in Fig. 4), implying a very broad crossover stretching over the full NSE time range.

How can we rationalize our results? In the literature on NC, a slowing down of the dynamics was attributed to (i) a glassy layer at the surface [24], (ii) slowing down because of a direct interaction with the surface [25], and (iii) an increasing of friction due to crowdedness at the particle surface [26,27]. None of these interpretations is compatible with the local dynamics results that show an unchanged local motion. Furthermore, Brownian dynamics simulations show that the difference between an end-fixed Rouse model and a model with a true reflecting wall are marginal [28]. As an explanation remains topological hindrance or crowding effects originating from the neighboring grafted chains. The surrounding end-connected chains cannot diffuse away, in order to make room for relaxation, and lead to topological hindrance. This may be nicely seen in comparing the chain relaxation within the corona of NP immersed in a matrix with that of the OCNC. At the crossover time $t_0 = 22.4$ ns, the mean squared displacement of the matrix chains amounts to $\langle r^2(t)\rangle = 2\sqrt{tWl^4/\pi} + 6D_R t \rightarrow \sqrt{\langle r^2(22.4\ \text{ns})\rangle} = 2.4$ or 2.1 nm originating from the internal chain modes. This may be compared with the distance between neighboring chains in a cone starting from the surface. For a representative 10 nm particle, the average distance between grafts is $d = \sqrt{\kappa^{-1}}$ with $\kappa = 0.5\ \text{nm}^{-2} \rightarrow d = 1.4$ nm, leading to a maximum distance at the outer rim of the shell ($t = 6$ nm) of $d_{\max} = 2.3$ nm corresponding very well to the motional distance at the crossover time. At longer times, the constraints from the other grafted chains become important, leading to a delay of interactions compared to the OCNC material: The interaction with other grafted chains is important for the topological effect, while the matrix chains may diffuse away and do not give rise to topological interactions. For the OCNC material, the chains are fully subject to constraints either by neighboring chains or by the interpenetrating chains from other grafted particles that all cannot diffuse away; employing the mode amplitude reduction factors A_p in Eq. (1), we may calculate the asymptotic motional range ($t \rightarrow \infty$) for a grafted chain as a function of the distance from the grafting point. The inset in Fig. 4 shows the result: The permitted fluctuation range of a grafted chain is confined by the cone, set by the next-nearest-neighbor grafted chains; only at the rim of the corona do the chain fluctuations very slightly exceed this limitation.

Thus, the dynamics of OCNC materials depends on topological features rather than on any changes on the segmental scale. For OCNCs, particle size and grafting density, determining the cone, are an important source for chain confinement. We have established this phenomenon

on unentangled Rouse chains. Longer grafted chains that carry entanglements would be the subject of a combination of the cone effect and the chain-chain entanglements; for long chains to first order, one might add these effects as $1/(d_{\mathrm{tot}}^2) = 1/(d_{\mathrm{cone}}^2) + 1/(d_{\mathrm{chain}}^2)$, with very significant ramifications on properties like toughness, fracture strength, etc., that were observed macroscopically [8,29]. Also, rheological properties are substantially enhanced.

*Present address: Institut für Organische Chemie, TU Clausthal, Leibnitzstrasse 6, 38678 Clausthal-Zellerfeld, Germany.

†Present address: Forschungszentrum Jülich GmbH, JCNS at SNS and Chemical and Engineering Materials Division, Oak Ridge National Laboratory (ORNL), 1 Bethel Valley Road, Oak Ridge, TN 37831, USA.

[1] M. Bockstaller, Prog. Polym. Sci. **40**, 1 (2015).
[2] D. Vlassopoulos and M. Cloitre, Curr. Opin. Colloid Interface Sci. **19**, 561 (2014).
[3] J. Che, K. Park, C. Grabowski, A. Jawaid, J. Kelly, H. Koerner, and R. Vaia, Macromolecules **49**, 1834 (2016).
[4] C. Grabowski, H. Koerner, J. Meth, A. Dang, C. Hui, K. Matyjaszewski, M. Bockstaller, M. Durstock, and V. R. A., ACS Appl. Mater. Interfaces **6**, 21500 (2014).
[5] E. Alonso-Redondo, M. Schmitt, Z. Urbach, C. Hui, R. Sainidou, P. Rembert, K. Matyjaszewski, M. Bockstaller, and G. Fytas, Nat. Commun. **6**, 8309 (2015).
[6] B. Iyer, V. Yashin, M. Hamer, T. Kowalewski, K. Matyjaszewski, and A. Balazs, Prog. Polym. Sci. **40**, 121 (2015).
[7] C. Deng, J. Wu, R. Cheng, F. Meng, H.-A. Klok, and Z. Zhong, Prog. Polym. Sci. **39**, 330 (2014).
[8] J. Choi, C. Hui, J. Pietrasik, H. Dong, K. Matyjaszewski, and M. Bockstaller, Soft Matter **8**, 4072 (2012).
[9] M. Schmitt, J. Choi, C. Hui, B. Chen, E. Korkmaz, J. Yan, S. Margel, O. Ozdoganlar, K. Matyjaszewski, and B. M. R., Soft Matter **12**, 3527 (2016).
[10] P. Voudouris, J. Choi, N. Gomopoulos, R. Sainidou, H. Dong, K. Matyjaszewski, M. Bockstaller, and G. Fytas, ACS Nano **5**, 5746 (2011).
[11] D. Dukes, Y. Li, S. Lewis, B. Benicewicz, L. Schadler, and S. Kumar, Macromolecules **43**, 1564 (2010).
[12] S. Milner, T. Witten, and M. Cates, Europhys. Lett. **5**, 413 (1988).
[13] C. Wijmans and E. Zhulina, Macromolecules **26**, 7214 (1993).
[14] G. Meyer, Ph.D. dissertation, University Münster, Germany, 2013.
[15] E. Hübner, J. Allgaier, M. Meyer, J. Stellbrink, W. Pyckhout-Hintzen, and D. Richter, Macromolecules **43**, 856 (2010).
[16] See Supplemental Material at http://link.aps.org/supplemental/10.1103/PhysRevLett.119.047801 for the particle details, SANS form factor, and local dynamics.
[17] A. Radulescu, N. Szekely, and M.-S. Appavou, J. Large-Scale Res. Facilities **1**, A28 (2015).
[18] N. Dan and M. Tirell, Macromolecules **25**, 2890 (1992).
[19] E. Mamontov and K. Herwig, Rev. Sci. Instrum. **82**, 085109 (2011).
[20] J. Wuttke *et al.*, Rev. Sci. Instrum. **83**, 075109 (2012).
[21] O. Holderer, M. Monkenbusch, R. Schätzler, H. Kleines, W. Westerhausen, and D. Richter, Meas. Sci. Technol. **19**, 034022 (2008).
[22] D. Richter, M. Monkenbusch, A. Arbe, and J. Colmenero, *Neutron Spin Echo in Polymer Systems*, Advances in Polymer Science Vol. 174 (Springer, Berlin, 2005).
[23] S. Hoffmann, L. Willner, D. Richter, A. Arbe, J. Colmenero, and B. Farago, Phys. Rev. Lett. **85**, 772 (2000).
[24] S. Y. Kim and C. F. Zukoski, Macromolecules **46**, 6643 (2013).
[25] F. Starr, J. Douglas, D. Meng, and S. Kumar, ACS Nano **10**, 10960 (2016).
[26] S. Cheng, S. Mirigian, J.-M. Y. Carrillo, V. Bocharova, B. Sumpter, K. Schweizer, and A. Sokolov, J. Chem. Phys. **143**, 194704 (2015).
[27] A. Ghanbari, M. Rahimi, and J. Dehghany, J. Phys. Chem. C **117**, 25069 (2013).
[28] C. Mark, Ph.D. dissertation, University Münster, Germany, 2013.
[29] J. Choi, H. Dong, and M. Bockstaller, J. Am. Chem. Soc. **132**, 12537 (2010).